1. Supporting Information

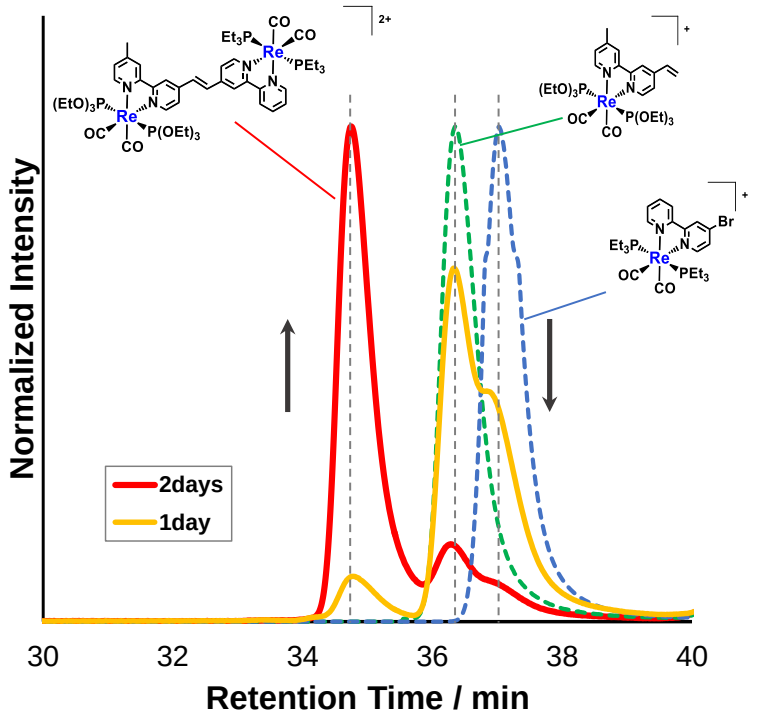

Fig. S1 SEC charts measured during synthesis of [**Re(OEt)Re(Et)**]$^{2+}$.

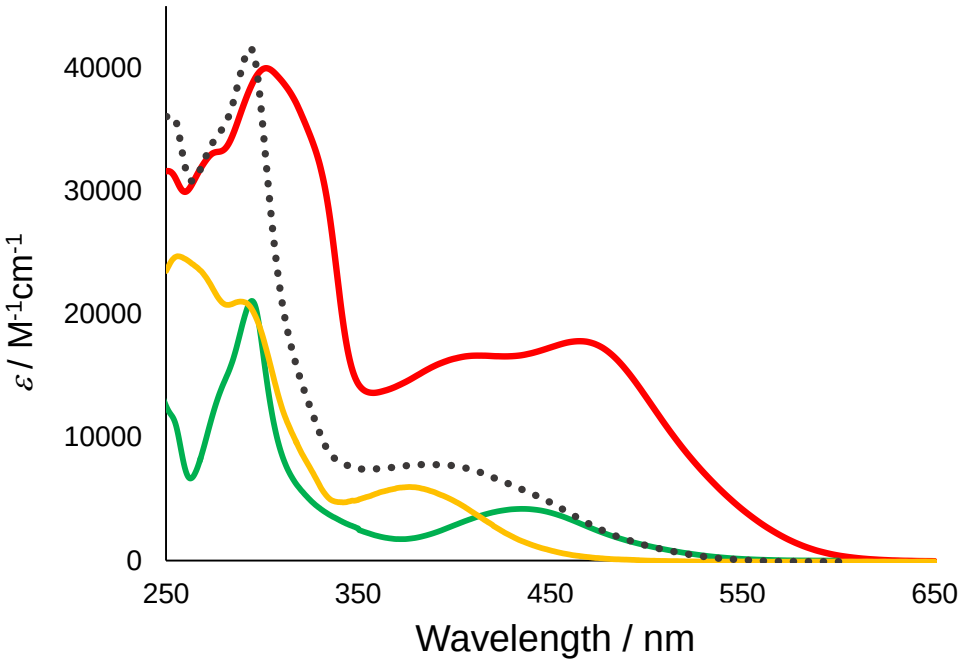

Fig. S2 UV-Vis absorption spectra of [**Re(OEt)Re(Et)**]$^{2+}$ (red), [**Re(C=C,OEt)**]$^{+}$ (yellow), [**Re(bpy)(CO)$_2$(PEt$_3$)$_2$**]$^{+}$ (green) measured in MeCN and 1:1 summation spectrum of [**Re(C=C,OEt)**]$^{+}$ and [**Re(bpy)(CO)$_2$(PEt$_3$)$_2$**]$^{+}$ (dotted line).

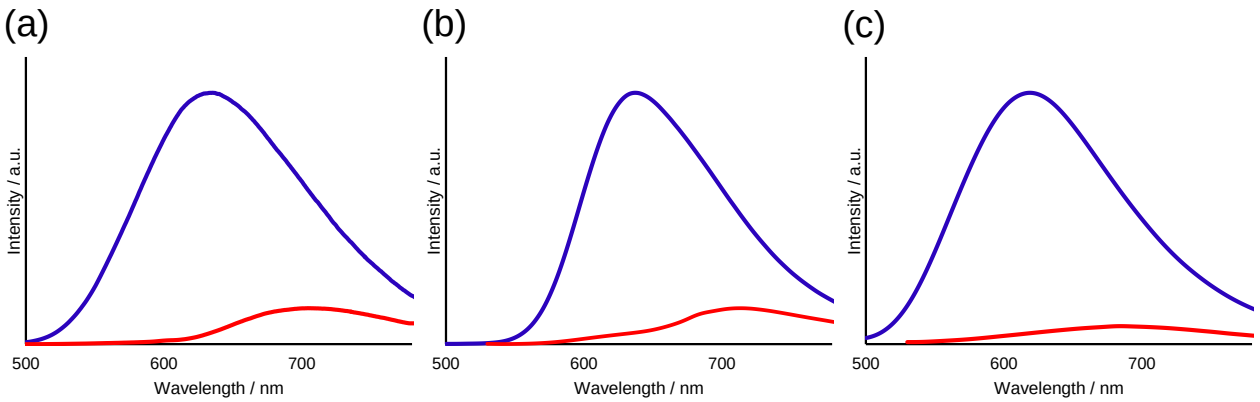

Fig. S3 Emission spectra of obtained trinuclear complexes and corresponding mononuclear complexes measured in MeCN. (a) **[Re(C=C,OEt)]**$^{+}$ (blue) and **[Re(OEt)$_2$Re(Ph)]**$^{3+}$ (red) (excitation wavelength: 444 nm). (b) **[Ru(C=C,bpy)]**$^{2+}$ (blue) and **[Ru(bpy)$_2$Re(Ph)]**$^{5+}$ (red) (excitation wavelength: 456 nm). (c) **[Ir(C=C,ppy)]**$^{+}$ (blue) and **[Ir(ppy)$_2$Re(Ph)]**$^{3+}$ (red) (excitation wavelength: 444 nm).

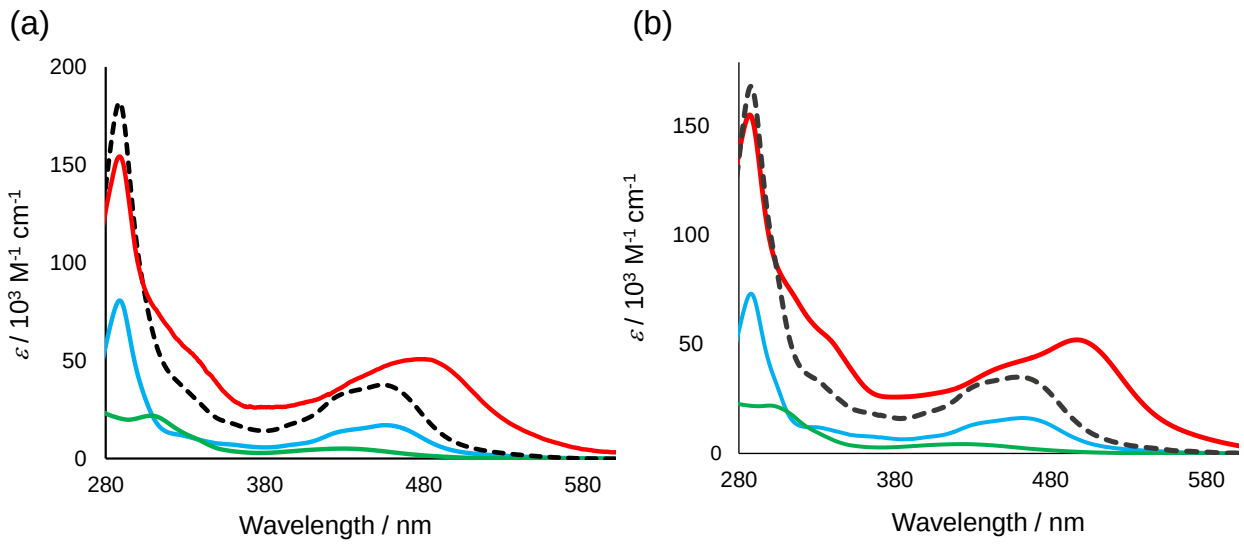

Fig. S4 UV-Vis absorption spectra of obtained trinuclear complexes and corresponding mononuclear complexes. The solvent was MeCN. (a) **[Ru(bpy)$_2$Re(Ph)]**$^{5+}$ (red), **[Ru(C=C,bpy)]**$^{2+}$ (blue), **[Re(C=C$_2$,Ph)]**$^{+}$ (green) and the 2:1 summation spectrum of **[Ru(C=C,bpy)]**$^{2+}$ and **[Re(C=C$_2$,Ph)]**$^{+}$ (dotted line). (b) **[Ru(dmb)$_2$Re(FPh)]**$^{5+}$ (red), **[Ru(C=C,dmb)]**$^{2+}$ (blue), **[Re(C=C$_2$,FPh)]**$^{+}$ (green) and the 2:1 summation spectrum of **[Ru(C=C,dmb)]**$^{2+}$ and **[Re(C=C$_2$,FPh)]**$^{+}$ (dotted line).

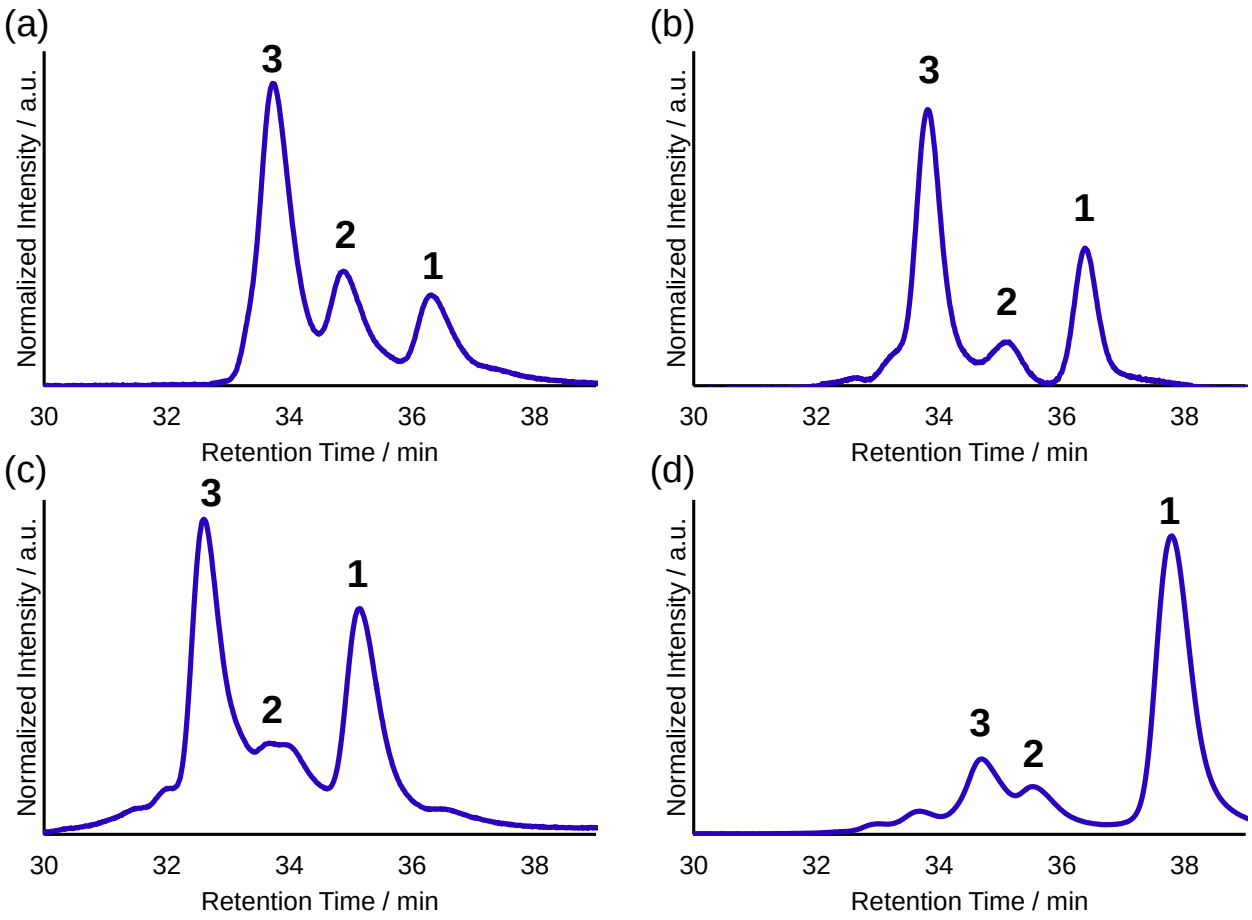

Fig. S5 SEC charts of the reaction mixture measured after the coupling reaction. (a) **[Re(OEt)$_2$Re(Ph)]$^{3+}$**, (b) [**Ru(bpy)$_2$Re(Ph)]$^{5+}$**, (c) [**Ru(dmb)$_2$Re(Ph)]$^{5+}$** and (d) **[Ir(ppy)$_2$Re(Ph)]$^{3+}$**. **1**, **2** and **3** in each figure represent the peaks attributed to mononuclear complexes, dinuclear complexes and trinuclear complexes, respectively.

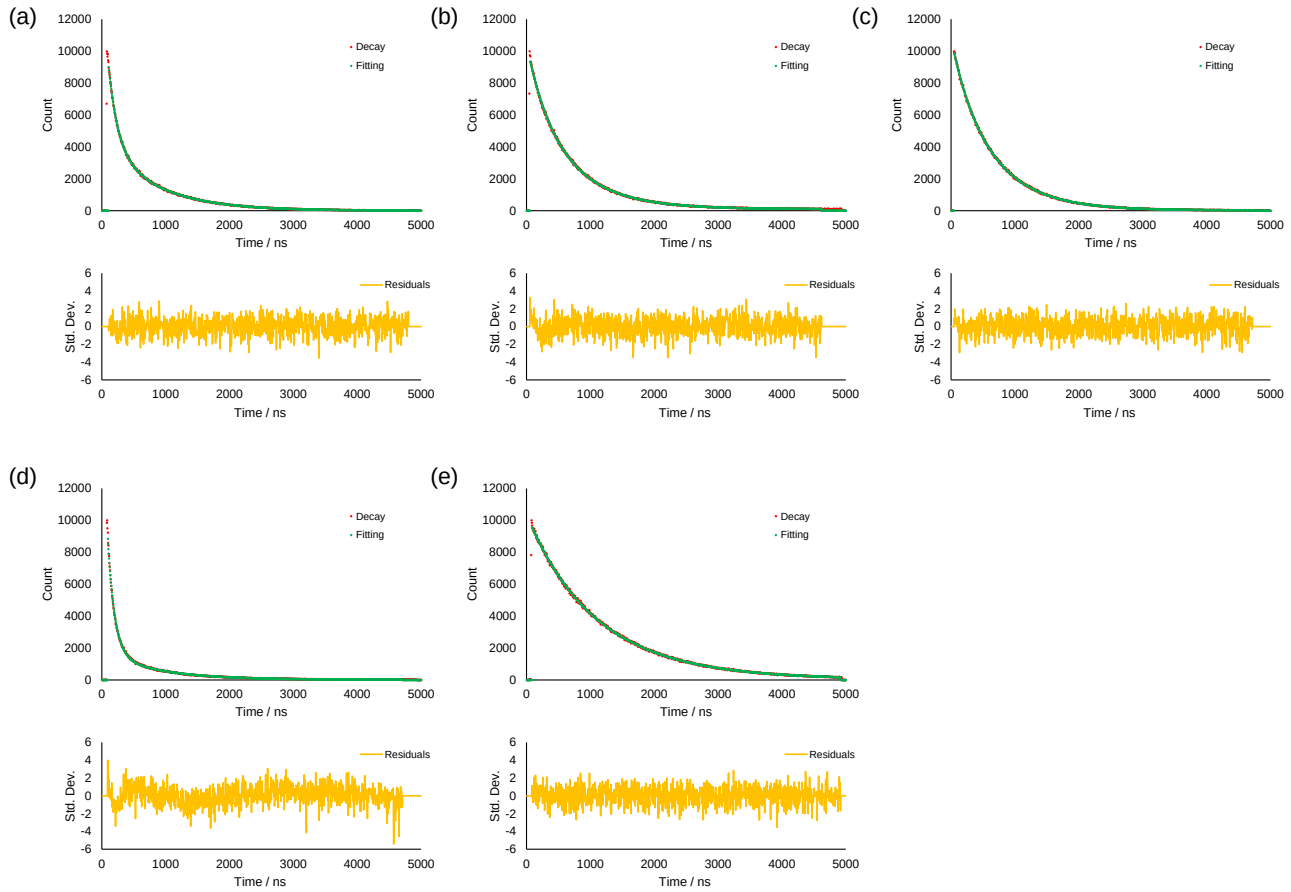

Fig. S6 Emission decays of obtained trinuclear complexes. (a) **[Re(OEt)$_2$Re(Ph)]$^{3+}$**, (b) **[Ru(bpy)$_2$Re(Ph)]$^{5+}$**, (c) **[Ru(dmb)$_2$Re(Ph)]$^{5+}$**, (d) **[Ir(ppy)$_2$Re(Ph)]$^{3+}$** and (e) **[Ru(dmb)$_2$Re(FPh)]$^{5+}$**. Dotted red lines show the observed decay curves and dotted green lines show the fitting curves with double exponential functions ($A_1\exp(-t / \tau_1)+A_2\exp(-t / \tau_2)$, where τ_i is the emission lifetime ($\tau_1<\tau_2$)). Orange lines show residuals between observed curves and fitting curves (χ^2: (a) 0.98, (b) 1.02, (c) 1.00, (d) 1.24 and (e) 0.99). Excitation wavelength was 444 nm for (a) and (d) and 456 nm for (b), (c) and (e). Detection wavelength was each wavelength of the emission maximum. The solvent was MeCN.

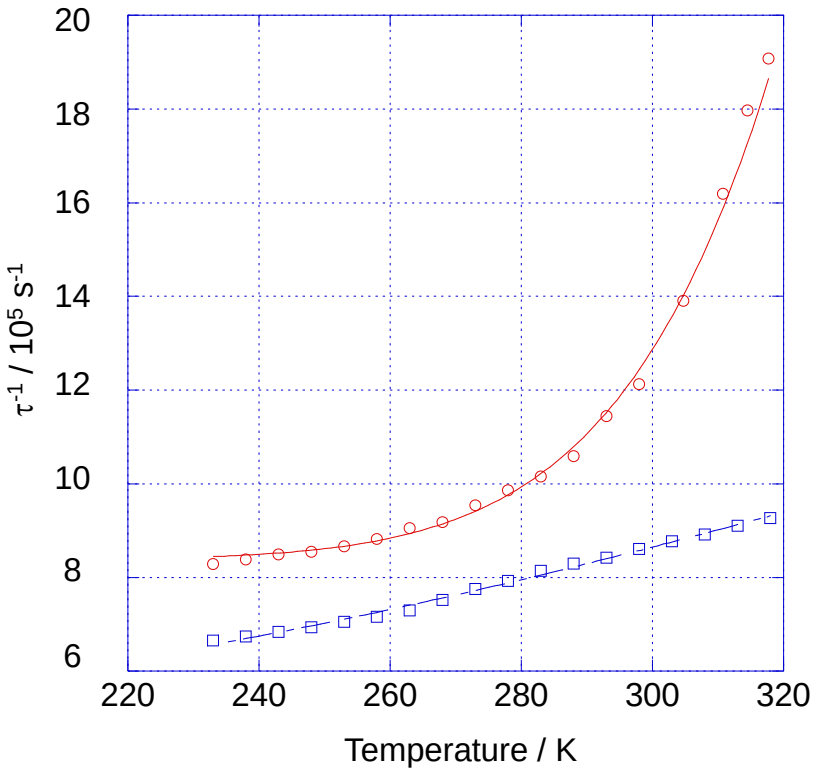

Fig. S7 Temperature dependence of **[Ru(dmb)$_2$Re(Ph)]$^{5+}$** (blue square) and [Ru(dmb)$_3$]$^{2+}$ (red circle). Excitation wavelength was 456 nm and detection wavelength was each wavelength of the emission maximum. The solvent was MeCN. The blue line and the red line show the fitting curves based on equation (1) below (**[Ru(dmb)$_2$Re(Ph)]$^{5+}$** ; k_r+k_{nr1}: 4.7×10^5 ± 0.37×10^5 s^{-1}, k_{nr2}: 7.1×10^6 ± 1.2×10^6 s^{-1}, ΔE: 580 ± 59 cm^{-1}, R^2: 0.99554. [Ru(dmb)$_3$]$^{2+}$; k_r+k_{nr1}: 8.4×10^5 ± 0.12×10^5 s^{-1}, k_{nr2}: 1.3×10^{12} ± 0.92×10^{12} s^{-1}, ΔE: 3100 ± 160 cm^{-1}, R^2: 0.99493)

$$\tau^{-1} = \frac{(k_{nr} + k_{nr1}) + k_{nr2}\exp(-\frac{\Delta E}{RT})}{1 + \exp(-\frac{\Delta E}{RT})} \qquad (1)$$

Table S1. Electrochemical properties of [**Ru(dmb)$_2$Re(Ph)**]$^{5+}$ and [**Ru(C=C,dmb)**]$^{2+}$ measured in DMF containing 0.1 M NEt_4BF_4 as an electrolyte.

Complex	potential in DMF, V (vs.Ag/$AgNO_3$)					
	$E^{red(5)}$	$E^{red(4)}$	$E^{red(3)}$	$E^{red(2)}$	$E^{red(1)}$	E^{ox}
Ru(dmb)$_2$Re(Ph)	-2.23 (78)	-1.95 (170)	-1.70 (70)	-1.48 (67)	-1.32 (68)	+0.73 (89)
Ru(C=C,dmb)	-2.20 (64)	-1.95 (68)		-1.72 (67)		+0.73 (76)